ISBN: 978-3-95450-210-3 doi:10.18429/JACoW-FEL2019-WEP054

BEAM DYNAMICS OPTIMIZATION OF A NORMAL-CONDUCTING GUN BASED CW INJECTOR FOR THE EUROPEAN XFEL*

H. Shaker†, H. Qian, S. Lal, G. Shu, F. Stephan, DESY, Zeuthen, Germany

Abstract

The European XFEL is operating up to 17.5 GeV electron energy with maximum 0.65% duty cycle. There is a prospect for continuous wave and long pulse mode (CW/LP) operation of the European XFEL, which enables more flexible bunch pattern time structure for experiments, higher average brightness and better stability. Due to engineering limitations, the maximum electron beam energy in the CW/LP mode is about 8.6/12.8 GeV [1], which puts more pressure on the injector beam quality for lasing at the shortest wavelength. This paper optimizes the beam dynamics of an injector based on a normal-conducting VHF gun.

INTRODUCTION

The European XFEL operates in the pulsed mode at the moment. The duration of each RF pulse is max. 650 µs and the repetition rate is 10 Hz. The time interval between bunches inside a pulse is 220 ns. This result to 27000 bunches per second and 0.65% duty cycle. For future development, the CW/LP mode operation is considered. Recent study shows a maximum 25 µA average current capability of SRF cavities in the European XFEL [1]. Based on this, the optimal value for the CW mode is selected to be 100 pC bunch charge with 4us bunch time interval. The maximum achievable energy is about 8.6 GeV for the CW mode. For the LP mode the energy can be increased to about 12.8 GeV [1]. More pressure on the beam quality is at the lower energy of the CW mode for lasing at short wavelengths. This requires better beam quality in comparison to the pulsed mode. The pulsed mode injector is based on a normal-conducting photo-cathode RF gun which is located in the XTIN1 tunnel [2]. To have the ability to work in dual modes, a new injector is required which will be placed in the XTIN2 tunnel on top of the XTIN1 tunnel. The second injector should have more or less the same energy as the first injector which is above 120 MeV [2,3]. To have a complete super-conducting machine, the first choice is a super-conducting gun. This kind of injector is under study and test [4]. As a backup solution a normal-conducting gun based CW injector is studied at PITZ [5,6]. CW Normal conducting photo-cathode RF guns were developed at LBNL in last decade based on mature room temperature RF technology [7], and the main limitation is the high average heat loss which limits both the achievable cathode gradient and the gap voltage. From DC to gigahertz frequency range, VHF band frequencies give us a reasonable cathode gradient, gap voltage and surface heat power. The successful CW APEX gun operates at 187 MHz, 20MV/m cathode gradient and 750KV gap voltage [7]. This gun is used as the electron source for LCLS-II at SLAC [8].

Based on the APEX experience, a 216.6 MHZ gun is under physics design at PITZ, and the cathode gradient and gun voltage are increased to 28 MV/m and 830 kV respectively[5, 6]. Besides, a 400 kV normal-conducting 1.3GHz buncher was developed [9]. To validate the gun and buncher design, a new injector dynamics optimization is presented in this paper. A multi-objective optimizer parallel processing code[10] based on the NSGA-II [11] algorithm is used to drive ASTRA [12] simulations for optimizing the injector.

MAIN BEAMLINE ELEMENTS

Figure 1 shows the conceptual beamline layout. To find the right amount of input parameters for the optimization algorithm we will talk about each component in the beamline. The initial laser beam has a flat-top longitudinal distribution with 2ps rise/fall time. The transverse distribution is Gaussian truncated at 1σ. The laser duration and radius are variable in the optimizer. Two cathode thermal emittances are assumed for injector optimizations: 1mm.mrad/mm for conservative case and 0.5mm.mrad/mm for optimistic case. The first case is close to the Cs_2Te cathode [13], and the second case is close to the multi-alkali cathode, such as K_2CsSb and NaKSb [14].

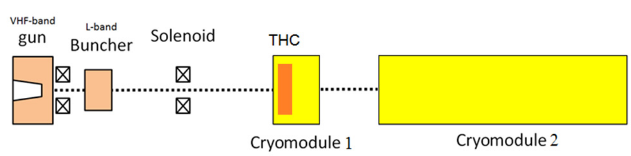

Figure 1: Beamline Layout

Gun and Main Solenoid

To minimize the emittance growth due to space charge, the electrons should be accelerated into the relativistic regime after photoemission as fast as possible. Then the maximum cathode gradient and gap voltage is desirable, but the average heat loss and the peak electric field on cavity surface limits the cathode gradient. Based on APEX gun experience, a maximum 100 kW heat loss and 30 MV/m peak surface field are considered as the baseline parameters. Due to these limitations a gun with 28 MV/m cathode gradient, 832 kV gap voltage and 3cm gap length was designed [5, 6]. Only the gun phase is variable during the beam dynamics optimization. The cathode position is assumed to be zero (z=0). The gun solenoid

* Work supported by the European XFEL
† hamed.shaker@desy.de

ISBN: 978-3-95450-210-3 doi:10.18429/JACoW-FEL2019-WEP054

should be as close to the cathode as possible, but without leaking high magnetic field onto the cathode. We fixed the solenoid central position at z=0.236 m. We used a solenoid profile designed by HZB, and its spherical aberration is 30% lower than the LCLS-II solenoid [15].

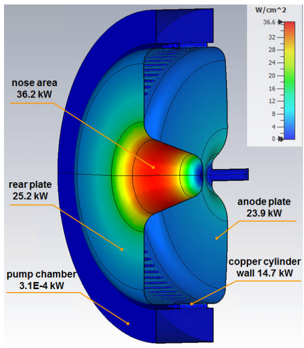

Figure 2: Gun Layout [6]

L-Band Buncher

The 1.3 GHz buncher is mainly for chirping the beam for velocity bunching, meanwhile it also accelerates the beam to reduce the space charge effect and thus reduce emittance growth. Figure 3 shows the current buncher design geometry and its axial electric field, more details of the buncher cavity design can be found in reference [9]. For the optimizer, the parameters we can play with are the RF input phase, total voltage up to 400kV (maximum achievable voltage) and also the buncher longitudinal position. The beam dynamics study shows better results for closer positions to the cathode but because of required components like main solenoid, vacuum valve and BPM, z=0.73m is the closest possible position.

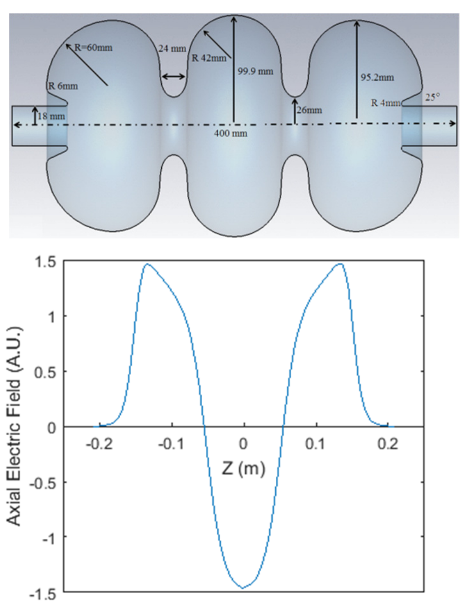

Figure 3: 1.3GHz buncher: geometry and axial field profile

Second Solenoid

The second solenoid is required for the matching of the beam to the following accelerating structure. For the optimizer, the longitudinal position and the current can be used. The result is not so sensitive to the solenoid position due to the preliminary beam dynamic study. Then with considering the required components between buncher and the cryomodule the longitudinal position is fixed to z=1.6m which is about in the center between cathode and the center of first accelerating cavity.

Accelerating Structures

In an initial study we worked with the standard XFEL cryomodule with eight 9-cell TESLA cavities but the result was not satisfying. By turning off the second and third cavities we reached some more satisfying result but the output energy was low (about 90 MeV). To resolve this problem we are using the same number of cavities inside two separate cryomodules for our model. The first cryomodule is smaller and has one or two cavities. The rest cavities are inside the second cryomodule. The distance between the cavity centers is 1.3848m in each cryomodule. For injector optimization, the amplitudes of the first two cavities are variable. For optimizing the velocity bunching, the phase of the first cavity is also allowed to vary. We put the rest cavities on-crest with maximum conservative amplitude of 32 MV/m. For future development, higher field up to 40 MV/m is planned [1]. Because of required components like laser window, BPM, vacuum valve etc between gun and booster linac, the minimum distance from cathode to the center of the first cavity inside the cryomodule 1 is set to 3 meter in optimizer. The drift between two cryomodules can also be optimized. Two cases are studied separately: 2+6 and 1+7 cavity cryomodules setup. Table 1 shows the best result we found for each case for 100pC bunch charge and 1mm.mrad/mm thermal emittance. Based on these results the 2+6 case is slightly better. To lower the total cost, it is better to use a standard X-FEL cryomodule instead of cryomodule 2 because of its availability. Then our models will be modified to 1+8 and 2+8 cavities with the same parameter values but with higher final energy. In this case we should consider the space availability in XTIN2 tunnel which gives us the 1+8 case as a more practical solution.

Third-Harmonic Cavity

Due to the nonlinear dynamics of velocity bunching in the low energy drift, the beam temporal profile gradually loses the flattop distribution, and develops a long tail at the injector exit. It's found most of the beam longitudinal asymmetry or skewness happens at the entrance of the cryomodule 1, because its RF phase is more close to on-crest phase and the beam gets a high 2nd order energy chirp. Similar to the phase space linearization for optimizing magnetic bunch compression, a harmonic cavity is introduced between buncher and the first cavity in cryomodule 1, as shown in Fig. 1, to symmetrize the beam longitudinal distribution. Figure 4 shows the longitudinal

ISBN: 978-3-95450-210-3 doi:10.18429/JACoW-FEL2019-WEP054

profile after and before symmetrisation using this cavity. The third case in table 1 shows the final beam parameters when it is longitudinally symmetrized. This cavity will be operated on 3.9 GHz with relatively small dimension and with the peak gradient about 8MV/m. Then it is so difficult to maintain it at resonance temperature in high average power CW operation and therefore it should be a super-conducting cavity. We propose to put this cavity inside the cryomodule 1.

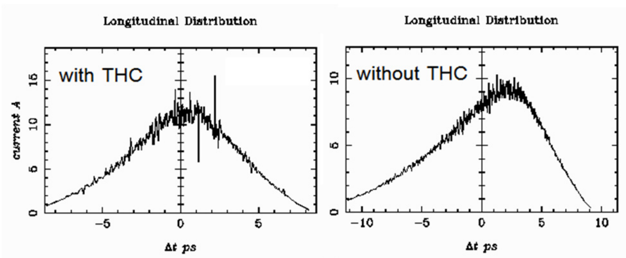

Figure 4: The effect of third-harmonic cavity to symmetrize the longitudinal profile

RESULTS AND SUMMARY

In last section we showed the result for 100pC bunch charge and 1mm.mrad/mm thermal emittance case which is valid for CS_2Te cathode [13]. We used the multi-objective evolutionary optimizer code [10] to minimize the transverse emittance and longitudinal bunch length. The optimizer gives us the Pareto front of optimal solution (see Fig. 5) and afterward in the post-processing we will select the solutions where the peak current is about 10A which is shown by the arrows in the Figure 5. The selected model was simulated again for finer mesh and more particles for more accurate results. We did the same for green cathodes such as K_2CsSb and NaKSb [14] with 0.5 mm.mrad/mm thermal emittance and the result is in the last column of Table 1. In this table just the higher order energy spread is mentioned because the first and second order energy spread will be minimized by the following accelerating structures and the third-harmonic cavity, respectively [16]. The higher order energy spread will remain and will be amplified by the following bunch compressors and reduce the final x-ray radiation brightness. All the rest beamline component parameters are mentioned in the table 2.

Table 1: Final Beam Parameters for Different Cases

Case	2+6	1+7	1+7 With THC	1+7 Green Cathode w/o THC
Emittance (100/95%) (mm.mrad)	0.19/0.13	0.19/0.14	0.18/0.14	0.13/0.09
Average sliced emittance (mm.mrad)	0.13	0.15	0.17	0.09
H.O Energy Spread (KeV)	2.9	2.2	2.7	2.8
Peak current (A)	11.5	10	11.5	10

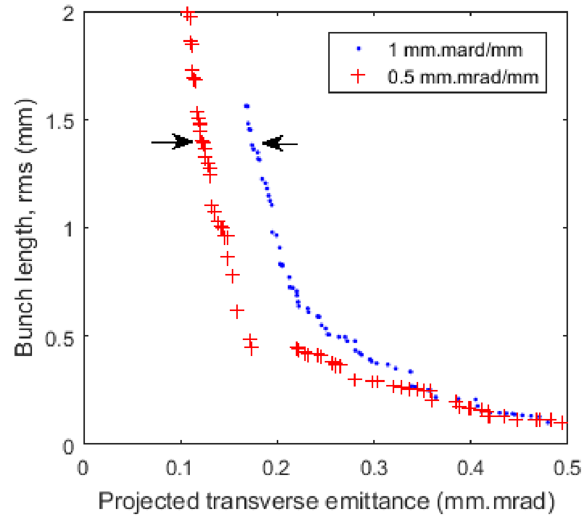

Figure 5: Pareto Front of optimizer for Cs_2Te and green cathode

Table 2: Final Beamline Components Parameters for Different Cases

Case	2+6	1+7	1+7 With THC	1+7 Green Cathode w/o THC
Laser spot size (mm)	0.24	0.26	0.28	0.26
Initial bunch length (ps)	51.5	45.6	40.0	47.8
Gun phase (deg)	3.1	-7.2	-1.1	-5.3
First (Second) Solenoid peak / Integral field (T/T.m)	0.058/ 0.0086 (0.036/ 0.0054)	0.060 /0.0090 (0.037 /0.0055)	0.062/ 0.0080 (0.032/ 0.0042)	0.060 /0.0089 (0.037 /0.0055)
Buncher Voltage (KV)	398	363	380	383
Buncher Phase (Deg)	-26.2	-35.8	-33.1	-32.2
First Cavity center (m) cryomodule 1/2	3.17/ 8.00	3.00 / 6.03	3.36/ 7.51	3.16 / 6.47
First/Second cavity max. field (MV/m)	23.52/ 29.36	23.18/ 3.80	21.14/ 25.11	23.67/ 22.45
First/Second cavity phase (deg)	-58.9/0	-29.7/0	-41.1/0	-36.5/0
Third-Harmonic cavity Max. field (MV/m)	0	0	8.1	0
Third-Harmonic cavity phase (deg)	0	0	180	0
Third-Harmonic cavity center (m)	0	0	1.8	0

ISBN: 978-3-95450-210-3 doi:10.18429/JACoW-FEL2019-WEP054

REFERENCES

[1] D. Kostin and J. Sekutowicz, "Ingredients for CW operation of SRF Linacs", Hamburg Alliance New Beams and Accelerators, DESY, Hamburg, September 2018.

[2] M. Altarelli *et al.,* "The European X-Ray Free-Electron Laser Technical design report", DESY 2006-097, July 2007, Ch. 7.

[3] F. Brinker, "Commissioning of the European XFEL Injector", in *Proc. 7th Int. Particle Accelerator Conf. (IPAC'16)*, Busan, Korea, May 2016, pp. 1044-1047. doi:10.18429/JACoW-IPAC2016-TUOCA03

[4] E. Vogel *et al.*, "SRF Gun Development at DESY", in *Proc. 29th Linear Accelerator Conf. (LINAC'18)*, Beijing, China, Sep. 2018, pp. 105-108. doi:10.18429/JACoW-LINAC2018-MOPO037

[5] S. Shu, Y. Chen, S. Lal, H. J. Qian, H. Shaker, and F. Stephan, "FIRST DESIGN STUDIES OF A NC CW RF GUN FOR EUROPEAN XFEL", in *Proc. 10th Int. Particle Accelerator Conf. (IPAC'19)*, Melbourne, Australia, May 2019, pp. 1698-1701. doi:10.18429/JACoW-IPAC2019-TUPRB010

[6] G. Shu, Y. Chen, S. Lal, H. J. Qian, H. Shaker, and F. Stephan, "Multiphysics Analysis of a CW VHF Gun for European XFEL", presented at the 39th Int. Free Electron Laser Conf. (FEL'19), Hamburg, Germany, Aug. 2019, paper WEP055.

[7] F. Sannibale *et al.*, Advanced Photoinjector Experiment Photogun Commissioning Results, PRST AB 15, 103501 (2012), doi.org/10.1103/PhysRevSTAB.15.103501

[8] LCLS-II Technical Design Report, T.O. Raubenheimer, ed. (2017).

[9] S. Lal *et al.*, "RF Design Studies of a 1.3 GHz Normal Conducting CW Buncher for European X-FEL", in *Proc. 10th Int. Particle Accelerator Conf. (IPAC'19)*, Melbourne, Australia, May 2019, pp. 3109-3111. doi:10.18429/JACoW-IPAC2019-WEPTS012

[10] C. F. Papadopoulos *et al.*, "Longitudinal and Transverse Optimization for a High Repetition Rate Injector", in *Proc. 36th Int. Free Electron Laser Conf. (FEL'14)*, Basel, Switzerland, Aug. 2014, paper THP057, pp. 864-867.

[11] K. Deb *et al.*, "A Fast and Elitist Multiobjective Genetic Algorithm: NSGA-II", IEEE Transactions on Evolutionary Computation (Volume: 6, Issue: 2, Apr 2002).

[12] K.Floettmann. ASTRA code. https://www.desy.de/~mpyflo/

[13] P. W. Huang *et al.*, "Test of Cs_2Te Thickness on Cathode Performance at PITZ", presented at the 39th Int. Free Electron Laser Conf. (FEL'19), Hamburg, Germany, Aug. 2019, paper WEP062.

[14] S.S. Karkare *et al.*, "Advances in Photocathode Technology at Cornell University", in *Proc. North American Particle Accelerator Conf. (NAPAC'13)*, Pasadena, CA, USA, Sep.-Oct. 2013, paper TUOAB1, pp. 391-393.

[15] Jens Völker, Private communications

[16] C.F. Papadopoulos *et al.*, "RF Injector Beam Dynamics Optimization for LCLS-II", in *Proc. 5th Int. Particle Accelerator Conf. (IPAC'14)*, Dresden, Germany, Jun. 2014, pp. 1974-1976. doi:10.18429/JACoW-IPAC2014-WEPRO015